Sulfur on $TiO_2(110)$ studied with resonant photoemission

E. L. D. Hebenstreit,[1,2] W. Hebenstreit,[1] H. Geisler,[3] S. N. Thornburg,[4] C. A. Ventrice, Jr.,[4] D. A. Hite,[5,6] P. T. Sprunger,[5,6] and U. Diebold[1]

[1]*Department of Physics, Tulane University, New Orleans, Louisiana 70118*

[2]*Institut für Allgemeine Physik, Vienna University of Technology, Wiedner Hauptstrasse 8–10, A-1040 Vienna, Austria*

[3]*Department of Chemistry, Xavier University of Louisiana, New Orleans, Louisiana 70125*

[4]*Department of Physics, University of New Orleans, New Orleans, Louisiana 70148*

[5]*Center for Advanced Microstructurs and Devices (CAMD), Louisiana State University, Baton Rouge, Louisiana 70806*

[6]*Department of Physics and Astronomy, Louisiana State University, Baton Rouge, Louisiana 70803*

(Received 23 February 2001; published 29 August 2001)

Adsorption of sulfur on $TiO_2(110)$ at room temperature (RT) and 350 °C has been studied with ultraviolet photoelectron spectroscopy. A $TiO_2(110)$ (1×1) surface with a small amount of oxygen vacancies was prepared by sputtering and annealing in ultrahigh vacuum. Oxygen vacancies induce a defect state that pins the Fermi level just below the conduction-band minimum. Sulfur adsorption at room temperature leads to the disappearance of this vacancy-related band-gap state, indicating that the surface oxygen vacancies are filled by sulfur. Sulfur-induced valence-band features are identified at binding energies of 3.4 and 8 eV. Adsorption of S at 350 °C forms a (4×1) superstructure at high coverages [$\approx$0.9 monolayer (ML)] that is visible with low-energy electron diffraction. In a previously proposed model for this superstructure, sulfur replaces half of the in-plane oxygen atoms and all the bridging oxygen atoms are removed. In agreement with this model, the oxygen 2*s* peak is decreased significantly and the defect state is increased. Two additional valence features are observed: one at 2.7 eV and one at 3.9 eV. Due to those features the band gap vanishes. In resonant photoemission, these features show a similar, but weaker, resonance profile than the vacancy-related defect state. Hybridized Ti-derived states extend across the whole valence-band region. Generally, a higher resonant photon energy is found for valence-band states with lower binding energies, indicating mainly $3p-4s$ transitions in the upper valence band. Adsorption of sulfur reduces the strength of the resonances.

DOI: 10.1103/PhysRevB.64.115418 PACS number(s): 68.47.Gh, 68.43.Fg, 79.60.−i

I. INTRODUCTION

Because sulfur is a common poison for catalytic reactions, the adsorption of sulfur compounds on metal and metal oxide surfaces has received considerable attention.[1,2] In particular, the adsorption of sulfur compounds on titanium oxides has been studied extensively.[3–8]

We have studied the interaction of elemental sulfur with the $TiO_2(110)$ surface. In our previous work we found three different adsorption sites for sulfur and a variety of structures with long-range order that depend on sulfur coverage and sample temperature during adsorption.[9,10] The experiments were performed with a clean UHV-annealed $TiO_2(110)$ surface that exhibits a few percent of oxygen vacancies [see Fig. 1(A)]. At low concentrations these vacancies are dispersed across the surface.[11] At room temperature scanning tunneling microscope (STM) studies indicate that sulfur binds to the titanium rows.[9] However, it could not be determined if the sulfur also adsorbs at the point defects. A very recent high-resolution photoelectron spectroscopy study indicates that this is the case.[12] Adsorption on the hot surface in the temperature range of 350−400 °C leads to the formation of a (4×1) superstructure at a coverage of $\approx$0.9 monolayer (ML). In Ref. 10 a model was proposed in which sulfur replaces 50% of the in-plane oxygen atoms while the bridging oxygen atoms are removed. In order to test this model and to clarify the binding sites for S adsorption at room temperature (RT), we performed photoemission measurements of the valence band and the shallow core levels.

Several photoemission studies of the clean $TiO_2(110)$ surface have been performed previously. In Refs. 13 and 14 the clean, almost stoichiometric surface was investigated, and the results were compared to *ab initio* calculations. For ob-

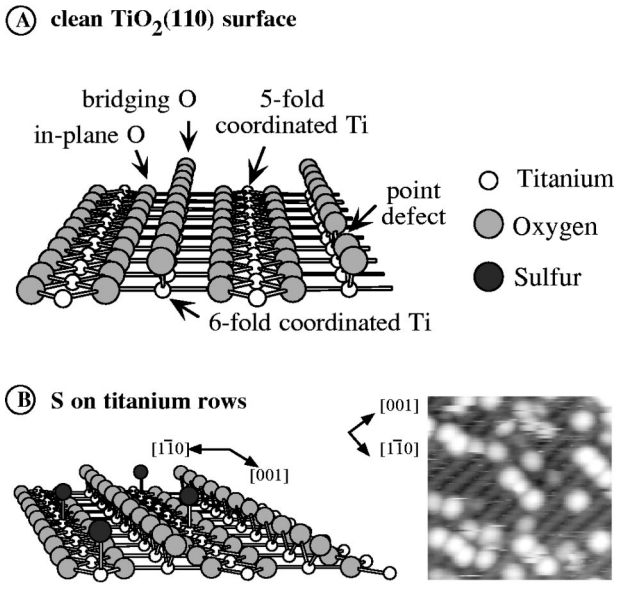

FIG. 1. (A) Atomic model of the clean $TiO_2(110)$ surface; (B) atomic model and STM image (95 Å × 95 Å, 1.4 V, 0.2 nA) of S adsorbed at RT on $TiO_2(110)$ (Ref. 9). The sulfur atoms, visible as white spots, are located on the bright titanium rows.

taining a deeper understanding of the interaction between titanium and oxygen, it is valuable to make use of the resonant photoemission effect for photon energies near the $3p-3d$ and $3p-4s$ transitions of Ti. This effect is explained in detail in Refs. 15 and 16. Resonant photoemission of the clean surface was studied by several groups[17–20] and film deposition of various elements was analyzed in Refs. 21–25. Additional investigations using resonant photoemission for Ti compounds were performed in Refs. 26 and 27. In this work we exploit the resonant photoemission effect to investigate the bonding between surface atoms and adsorbates. The measurements were performed with photon energies of 29–94 eV, covering the range for the $3p-3d$ and $3p-4s$ transitions in Ti.

Because resonant photoemission has already been explained in detail in the references mentioned above, we only summarize briefly the main concept. It is based on the quantum-mechanical interference between two excitation processes that transform a certain initial state to the same final state via two different pathways.

The direct photoemission process produces electrons with the kinetic energy E:

$$3p^6 3d^n + h\nu \Rightarrow 3p^6 3d^{n-1} + e^-(E). \quad (1)$$

Concurrent to Eq. (1), optical adsorption may lead to excitation of the $3p$ to the $3d$ (or $4s$) level:

$$3p^6 3d^n + h\nu \Rightarrow [3p^5 3d^{n+1}]^*. \quad (2)$$

The excited state decays and an electron is emitted with the same kinetic energy as for process (1):

$$[3p^5 3d^{n+1}]^* \Rightarrow 3p^6 3d^{n-1} + e^-(E). \quad (3)$$

For photon energies in the resonant region, the peak intensity should exhibit a characteristic, asymmetric peak shape (Fano profile).[15] In relatively light transition metals such as Ti, additional excitations accompany the optical adsorption causing changes in the resonance.[26] In addition, the resonance is moved to higher photon energies than expected from the separation of the contributing energy levels (approximately 47 eV for the $3p-3d$ transition instead of 33 eV) due to the exchange interaction between $3p$ and $3d$ levels.[16]

Because the photoexcitation and recombination process is spatially localized, resonant emission in the mainly O $2p$ derived valence band is only possible if oxygen states are strongly hybridized with the titanium orbitals. This is the case for the Ti–O bonds of $TiO_2(110)$ and resonant photoemission is found for the whole valence band.[17] In a molecular-orbital picture bonding orbitals with strong Ti $3d$ character dominate at higher binding energy. For lower binding energy, nonbonding orbitals with mainly O $2p$ contribution are found.[18] The minimum peak intensity for resonant photoemission is found at a photon energy of approximately 36 eV. A resonant enhancement is found up to photon energies of approximately 60 eV.

II. EXPERIMENTAL PROCEDURE

The measurements were performed at the Center for Advanced Microstructures and Devices (CAMD) on the PGM beamline. The angle resolved photoemission spectra were taken at normal emission with *p*-polarized light. The angle of incidence of the photon beam was 45°. The photon energy ranged between 29 and 95 eV. All spectra were normalized to the photon flux using a tungsten grid placed within the optical beam path. The Fermi level was calibrated by measurements of the Fermi edge of a piece of Ta in electrical contact with the sample.

All measurements were carried out on a dark blue TiO_2 crystal that was reduced by heating up to 700 °C for several hours. The sample was cleaned by ion bombardment with 1-keV Ne^+ ions at room temperature and subsequent annealing in UHV for 10 min at 650 °C. This sample treatment produces a (1×1) surface which exhibits point defects with a density of a few percent.[11] The base pressure in the preparation chamber was in the low 10^{-10}-mbar range.

The elemental sulfur was produced by electrolytical dissociation of Ag_2S in a sulfur cell. The cell was constructed as described in Ref. 28. The cell itself was constantly heated to a temperature in the range of 150−165 °C. The dosing procedure is described in detail in Ref. 10. A coverage of one monolayer is defined as one S atom per substrate unit cell.

The photoemission measurements were performed at RT after adsorbing a saturation coverage of S on the clean surface. According to previous low-energy electron diffraction (LEED) and STM measurements no superstructures are formed by S when adsorbed at RT.[9,10] To minimize the effect of photoinduced desorption during the measurements of S when adsorbed at RT, the sample was moved laterally after taking 2–3 spectra. For adsorption of S at 350 °C, the formation of a (4×1) superstructure was confirmed with LEED before taking the photoemission spectra. No photoinduced desorption was found during the photoemission measurements from this superstructure. Upon normalization to the photon flux the analysis of all spectra was done after substracting an integrated background (Shirley background) to account for the inelastically scattered electrons. Only the spectra in Figs. 3 and 11 are presented without background substraction.

III. RESULTS

A. Valence-band spectra of S/TiO_2(110) adsorbed at RT

An STM image for S/TiO_2(110) adsorbed at RT is shown in Fig. 1(B) together with a geometric model that is based on previous results.[9] Sulfur adsorbs on the bright titanium rows as indicated in the model in Fig. 1(B). Usually a few percent of point defects (i.e., missing bridging oxygen atoms) are present on the surface after annealing in UHV [see Fig. 1(A)], and are known to be very active sites for adsorption. Generally, defects are imaged as bright spots on dark rows. However, depending on the tip state, they may not always be visible.[11] This makes a statistic evaluation of defect sites in STM images difficult. In addition, sulfur atoms appear as very large protrusions, possibly shielding neighboring va-

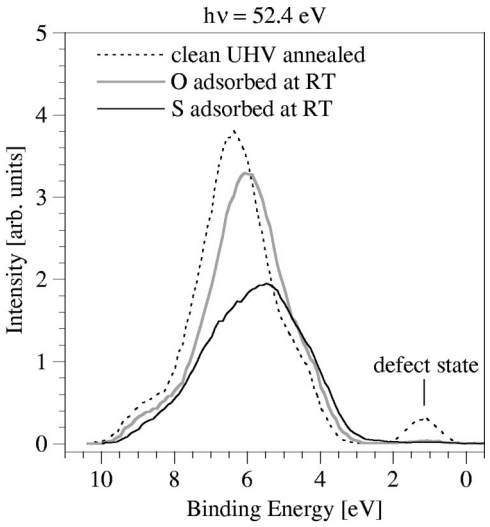

FIG. 2. Photoemission spectra of the valence band (normal emission) of TiO_2(110) at $h\nu = 52.4$ eV (in resonance). Annealing in UHV creates point defects in the rows of bridging oxgyen as indicated by the defect state in the band gap. The defect state disappears when sulfur or oxygen is adsorbed at RT. Adsorption of oxygen and sulfur adsorption at room temperature cause a rigid shift of the spectra to lower binding energy by 0.2 and 0.4 eV, respectively.

cancy sites, and are quite mobile when adsorbed at room temperature. Therefore STM alone is insufficient to decide if these vacancies are possible S adsorption sites. Photoemission experiments of the valence band (VB) are well suited to address this question. The presence of oxygen defects on the TiO_2(110) surface leads to an excess of electrons in the neighborhood of the defect that results in a defect state (labeled g_1 in the photoemission spectra shown below) within the band gap. The formal oxidation state of the titanium cations next to a defect is reduced from 4+ to 3+. It is known that O_2 adsorbs dissociatively at RT at oxygen vacancies and fills these defects.[29] The adsorption process is not precursor mediated, i.e., only these oxygen molecules that directly hit a vacancy dissociate and adsorb on the surface by occupying the defects. When oxygen is dosed at room temperature the surface remains unchanged except for the population of the defects.

Photoemission spectra of the VB region were measured before and after sulfur and oxygen adsorption at RT. In Fig. 2 three spectra from three differently prepared surfaces are compared at a photon energy of 52 eV, which is within the range of the Ti resonance energies. At this photon energy, the defect state within the band gap is enhanced due to $3p-3d$ excitation and can be compared more easily for the different surfaces. The VB of the clean UHV annealed surface shows a defect state at approximately 1.1 eV below the Fermi level. After dosing 210 Langmuire (L) molecular oxygen at RT the defect state (see Fig. 2) has almost completely vanished, in agreement with the expected filling of oxygen vacancies on the surface at RT. Adsorption of S at RT on the clean UHV annealed surface leads to similar results. The defect state has completely vanished after exposure to less than 100 L. According to previous experiments this exposure is sufficient to produce a saturation coverage which is about 0.7 ML for adsorption of S at RT. This indicates that S occupies the defects (see Sec. IV A), in addition to the titanium rows shown in Fig. 1(B).

Another effect that is seen in Fig. 2 is the shift of the whole VB for S and O_2 adsorption at RT as compared to the clean UHV annealed surface. The shift to lower binding energies for S is about 0.4 eV and for O at RT it is in the range of 0.2–0.3 eV. This shift is most likely caused by a band bending effect[30] as discussed in Sec. IV A.

The intensity of the VB emission was significantly lowered by the adsorption of sulfur at both RT and 350 °C. The primary reason for this phenomenon lies in the different photoionization cross sections of sulfur and oxygen. The atomic cross section for photoionization of the O $2p$ orbital at a photon energy of 40.8 eV is 6.8×10^6 b.[31] For the same photon energy the cross section for ionizing the S $3p$ orbital in a S atom is ten times lower with 0.6×10^6 b. The kinetic energy of the photoelectrons in our spectra are close to the minimum of the well-known universal curve for inelastic mean free path lengths, which ensures a high surface sensitivity. The presence of S causes inelastic scattering of the photoelectrons from the underlying layers (thus attenuating the valence band), and any new features related to the S $3p$ peak are very weak because of the low cross section.

To investigate how sulfur adsorption at different sites influences the valence band, sulfur was adsorbed at RT on the clean surface with and without oxygen defects. The defect-free surface was prepared by first dosing oxygen at RT on a clean, UHV annealed surface that exhibited the defect state. Both adsorption experiments provide surfaces with sulfur adsorbed on the titanium rows. The only difference is that in the first case the defects are filled by sulfur while in the second case the defects are occupied by oxygen. Comparison between the valence bands of these two surfaces in a photon energy range from 34 to 74 eV shows no significant differences in the spectra (spectra not shown).

In order to analyze the valence-band features that are caused by sulfur adsorption on the fivefold coordinated Ti atoms, we adsorbed S on the defect-free surface and compared it with the clean defect-free surface. Again, the defect-free surface was prepared by UHV annealing with subsequent adsorption of oxygen at RT. The complete series of valence-band spectra for the defect-free surface and S at RT are presented in Figs. 3(A) and (B). The valence emission of the clean defect-free surface and the surface after sulfur adsorption are shown Fig. 4 for a photon energy of 39 eV, which is below resonance. For easier comparison the curve after S adsorption is shifted by 0.2 eV to higher binding energies to compensate for band bending effects and ensure an overlap of the valence bands in the graph. At least five different peaks could be distinguished in the valence band for both surfaces. The peak positions in the case of sulfur adsorption (after the 0.2-eV shift) are at 4.3–4.6 eV (A), 5.3–5.6 eV (B), 6.5–7 eV (C), 7.5–8 eV (D), and 8.5–9 eV (E) plus an additional shoulder around 3 eV, see the labels on the spectrum for $h\nu = 38.7$ eV in Figs. 4 and 3(B). (For some photon energies it was difficult to identify the features. We therefore give a range for the binding energy of the different

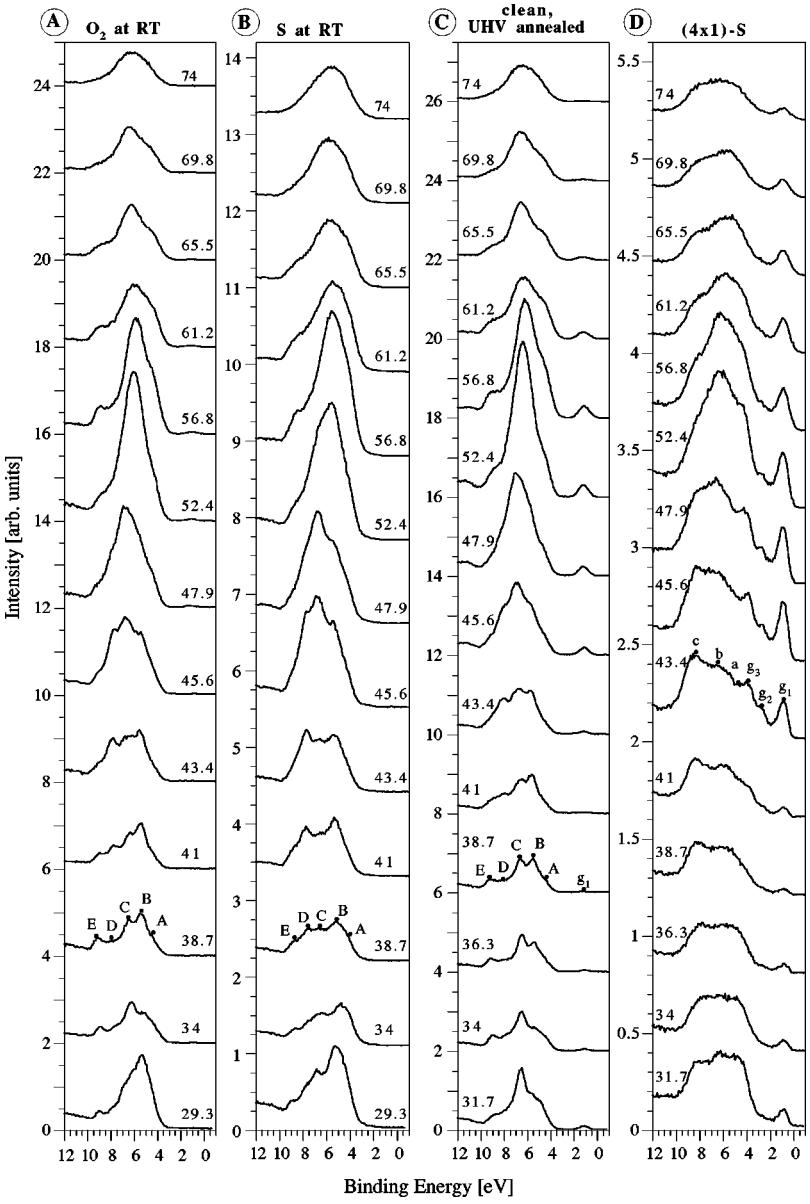

FIG. 3. Photoemission spectra of the valence band (normal emission) of differently prepared $TiO_2(110)$ surfaces. (A) After oxygen adsorption at RT (defect-free surface), (B) after S adsorption at RT on the defect-free surface, (C) the clean UHV annealed surface, and (D) the (4×1)–S superstructure produced by S adsorption at 350 °C. The labeled black dots indicate peaks analyzed in Figs. 5 and 9.

peaks. This accounts for dispersion as well as the uncertainy in the determination of the accurate peak position.) The peak positions for the defect-free clean surface (oxygen adsorption at RT) are within the same range as for sulfur except for peak C which is located at slightly lower binding energies around 6.3 eV. This stands in good agreement to the values in Ref. 14 for a clean surface with very few oxygen defects. At some photon energies an additional shoulder at 7 eV becomes visible but it never appears as distinct peak.

Despite the low cross section for photoemission from S $3p$, two features are identified in Fig. 4 as being caused by S adsorption. The first one is a small shoulder at around 3 eV, which appears at the valence-band maximum of TiO_2. This region shows a somewhat higher intensity for all photon energies as compared to the clean surface. In a photoemission study of $Ti_{1+x}S_2$ (Ref. 27) the emission from S $3p$ orbitals is assigned to a peak at a binding energy of 3.4 eV as well as intensity in the regions around 2.2 and 5 eV. The shoulder in Fig. 4 at 3 eV can therefore be related to a sulfur $3p$ feature. The second S-related feature in our spectra is located around 8 eV. This is the only binding-energy region within the valence band where the emission from the sulfur covered surface for low photon energies (<48 eV) is clearly higher than for the clean surface. The ratio of the valence-band emission for S adsorption/O adsorption exhibits a peak around a binding energy of 8 eV for all photon energies. This is an additional indication for a S-related emission in this area.

To estimate the resonant behavior of the various features in the valence band, the peak heights were plotted against photon energy. In Ref. 18 the valence band was fitted with three Gaussians, attributed to bonding and nonbonding orbitals as well as ''overlap'' and the intensity variation as a function of photon energy was followed. The angle-resolved spectra presented in this work show much more structure; therefore peak fitting would clearly be unreasonable. However, we are aware that using peak heights is a rough approximation, and only the general trends of the valence-band resonances will be deduced from the results. The peak

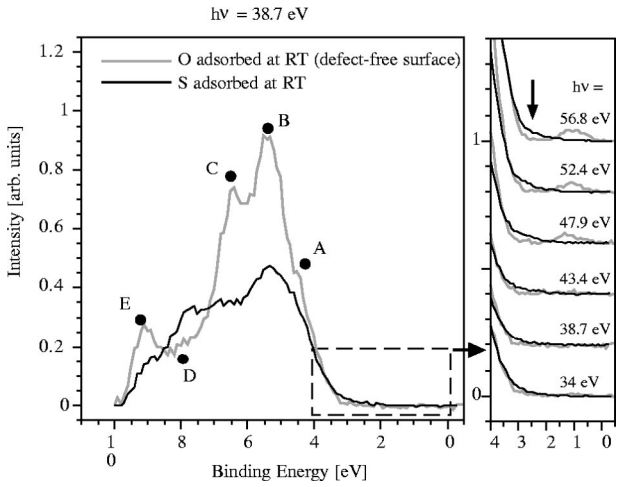

FIG. 4. Photoemission spectra of the valence band (normal emission) of TiO_2(110) at $h\nu = 38.7$ eV (below resonance). The spectrum with adsorbed S is shifted by 0.2 eV to higher binding energy to compensate band bending effects and to facilitate comparison of the two spectra. The right plot shows the small shoulder at 3 eV for different photon energies.

heights of the valence-band features A–E for the clean defect-free surface after adsorption of oxygen at RT are shown in Fig. 5(A). The corresponding plots for the sulfur-covered surface are shown in Fig. 5(B). In Fig. 5(B) all peaks show resonances at different energies. There appears to be a general trend that peaks at higher binding energies show a maximum in the resonance profile at lower photon energies. Only the peak at 8.9 eV represents an exception with an additional maximum at higher photon energies. The photon energy dependence of the S shoulder at 3 eV was not plotted. Because of the small peak size and overlap with the VB a

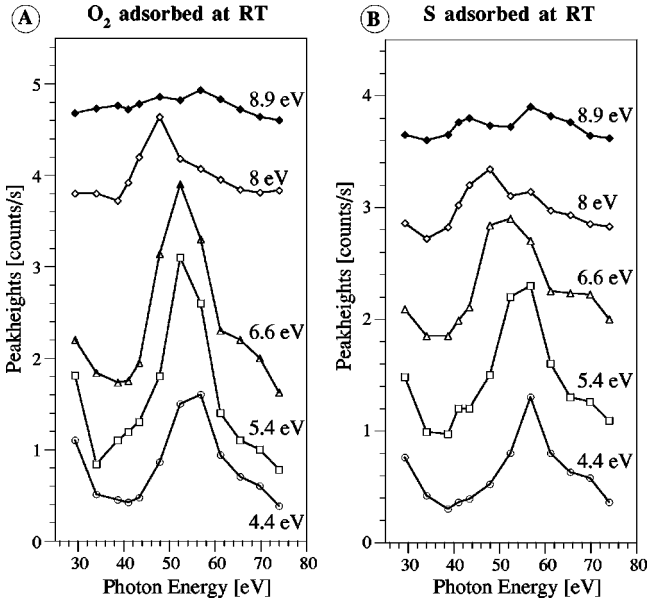

FIG. 5. Peak heights of selected features in the valence band [see Figs. 3(A) and (B)] versus photon energy. (A) Adsorption of oxygen at RT. (B) Adsorption of sulfur at RT on the defect-free surface. The curves are offset for clarity.

	Peak height at resonance / Peak height below resonance				
Peak at respective BE (s.text)	O at RT	S at RT	Clean UHV annealed	S(4 × 1)	
				BE [eV]	Ratio
g_1			16	0.9 (g_1)	10.4
band gap				2.6 (g_2)	5.2
band gap				3.6 (g_3)	4.1
A	3.6	4.3	4.2	4.8 (a)	2.7
B	4.5	3.8	4.9		
C	4	4	4.7	6.3 (b)	3.2
D	5.2	3.8	5.5	8.1 (c)	2.1
E	2	4	2.4		

FIG. 6. Ratio of peak heights in resonance to peak heights below resonance ($h\nu$ between 34 and 39 eV) for features A–E (see Fig. 5), the defect state g_1 of the clean surface (Fig. 10) and the (4×1)–and S superstructure [see Figs. 3(D) and 9].

detailed evaluation was not possible. It appeared, however, that this peak does not have the resonant behavior of the rest of the valence band.

The spectra from the clean surface in Fig. 5(A) show a similar photon energy dependence as the spectra after adsorption of sulfur at RT. Differences are found mainly for the peaks with the highest intensity, located around 5.4 and 6.3 eV. After sulfur adsorption the peak at 5.4 eV is higher than the peak at 6.3 eV for most photon energies. For the clean surface both peaks show a similar intensity. The peak at 8 eV, which is assigned at least partially to emission from sulfur, shows a resonant behavior similar to the clean surface. As a measure for the strength of the resonances, we calculated the ratio between the peak height in resonance and the peak height at a photon energy of 34 eV (near the minimum in the resonance) for each peak. Figure 6 gives the values for the respective peaks.

B. Valence-band spectra of the TiO_2(110) (4×1)–S superstructure

High coverages of sulfur adsorbed at 350 °C (saturation coverage approximately 1 ML) lead to the formation of a (4×1) superstructure. A model has been proposed in our previous work,[10] which is consistent with the STM, x-ray photoelectron spectroscopy (XPS), and LEED results. An STM image of the superstructure and the model is shown in Fig. 7. The bridging oxygen atoms are removed and 50% of the in-plane oxygen atoms are replaced by sulfur. Detailed explanations of this model can be found in Ref. 10. In the following, some aspects of this model are investigated with surface sensitive photoemission spectra.

The removal of the bridging oxygen atoms induces a change in the coordination number of the neighboring Ti atoms as compared to the clean surface. When a single oxygen atom is missing from the clean surface the coordination number of the Ti atoms underneath the vacancy changes from 6 to 5. For Ti atoms underneath the former bridging

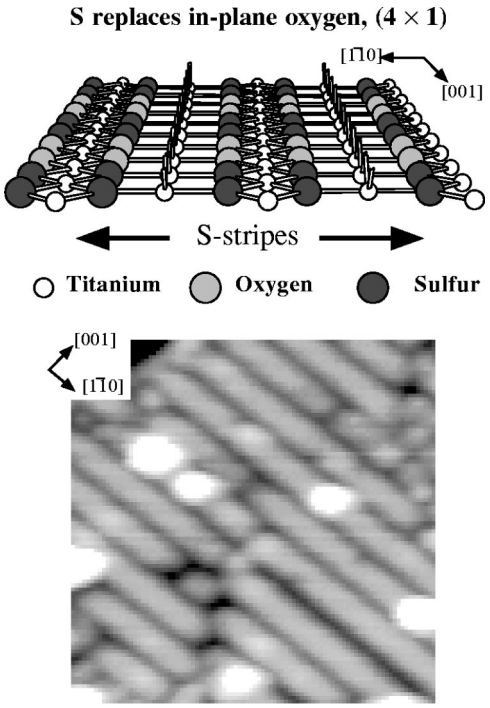

FIG. 7. Atomic model and STM image (92 Å × 92 Å, 1.6 V, 0.3 nA) of the $TiO_2(110)$ (4×1)−S superstructure that forms when S is adsorbed at 350 °C on $TiO_2(110)$ (Ref. 10). Sulfur replaces 50% of the in-plane oxygen atoms. All the bridging oxygen atoms are missing. The bright rows in the STM image represent the sulfur stripes.

oxygen rows in the (4×1) superstructure, the coordination number changes to 4. In addition, a large number of oxygen atoms are replaced by the less electronegative sulfur. Both the coordinative undersaturation and the less electronegative ligands cause a reduction of the Ti^{4+} atoms as evidenced in strong Ti^{3+} shoulders in XPS from the (4×1)−S surface.[10] It should also give rise to a change in the defect state in the band gap. Generally, the removal and replacement of the surface oxygen atoms should be visible in the form of a smaller 1*s* or 2*s* oxygen peak. With XPS only a very small decrease of the O 1*s* peak was found in previous measurements.[10] Because the XPS signal at a binding energy of 530 eV (kinetic energy of 720 eV for Mg-$K\alpha$ line) comes from several atomic layers this result does not exclude an oxygen depletion of the topmost layer. Synchrotron-based ultraviolet photoemission measurements, which are more surface sensitive, should show if the conjectured depletion of surface oxygen indeed takes place.

The valence-band spectra of the clean UHV annealed surface and the surface after dosing sulfur at 350 °C are shown in Fig. 8 for two different photon energies. The photoemission spectra in graph (A) were taken at a photon energy of 38.7 eV (below resonance) while graph (B) was measured with a photon energy of 47.9 eV (in resonance). The valence band of the (4×1) superstructure is changed dramatically as compared to the clean UHV annealed surface. Two new peaks at around 2.7 and 3.9 eV [visible more clearly in graph (B), labeled as g_2 and g_3] appear in the band-gap region of the clean TiO_2.

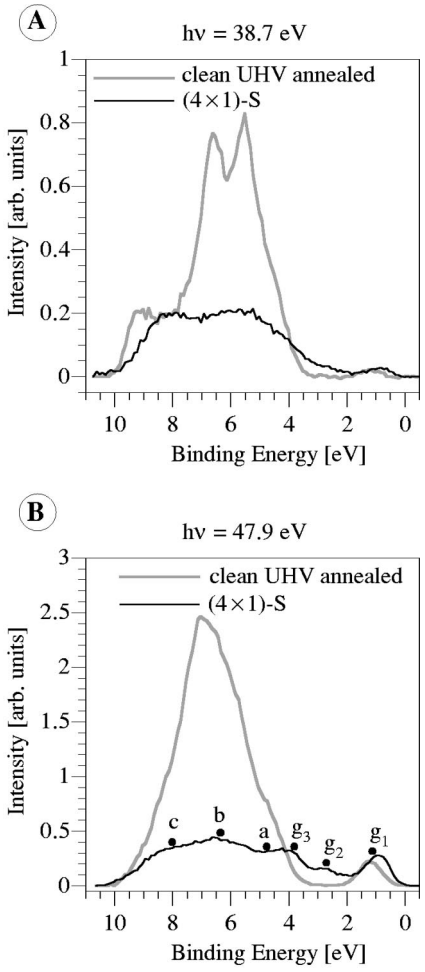

FIG. 8. Comparison between photoemission spectra of the valence band (normal emission) of a clean UHV annealed $TiO_2(110)$ and after adsorption of S at 350 °C [(4×1)−S superstructure]. (A) $h\nu=38.7$ eV (below resonance) and (B) $h\nu=47.9$ eV (in resonance).

The attenuation of the valence band caused by sulfur in the (4×1) structure is much higher than for sulfur adsorption at RT. The higher saturation coverage in comparison to adsorption at RT, combined with the low photoionization cross section of sulfur, leads to the weak emission from the VB. For some photon energies, the intensity of the VB is only 1/5 of the intensity of the clean surface.

The ratio of the valence bands of the (4×1)−S surface to the clean surface shows the smallest attenuation for binding-energies around 8 eV, similar to adsorption of S at RT. This would again point to sulfur derived emission in this binding-energy region.

The defect state g_1 of the (4×1)−S superstructure is located at approximately 0.3 eV lower binding energy than for the clean surface. The emission from the defect state as well as the states g_2 and g_3 are significantly increased for resonant photon energies. To provide an overview of the resonance behavior of spectra from the (4×1)−S surface, valence-band spectra are shown in comparison with the clean UHV annealed surface for photon energies between 31.7 and 74 eV in Figs. 3(C) and (D).

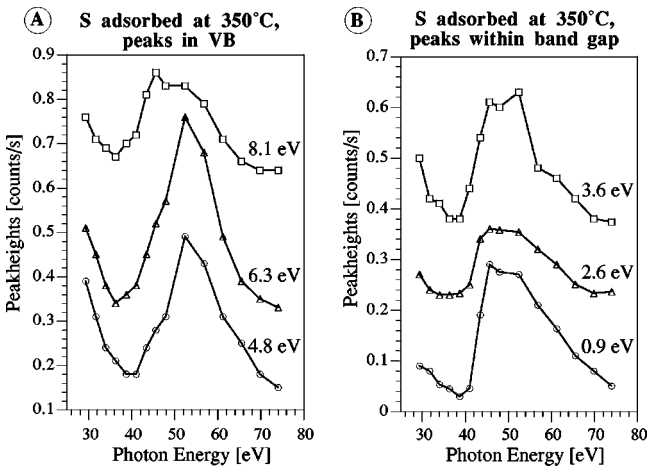

FIG. 9. Peak heights of valence-band peaks at selected positions [see Fig. 3(D)] versus photon energy for the (4×1)–S superstructure. (A) Three positions in the valence band (a–c), (B) band-gap states. The curves are offset for clarity.

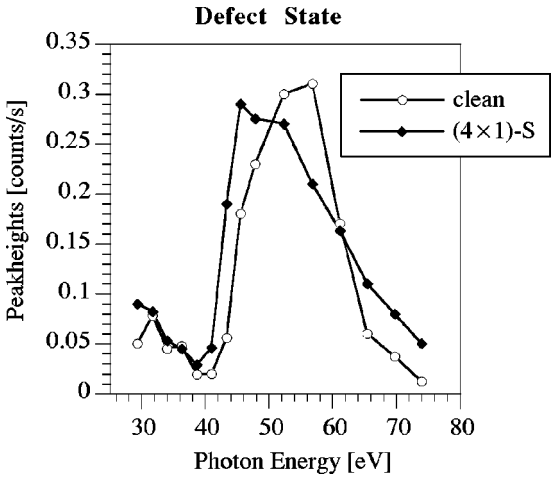

FIG. 10. Peak heights of the g_1 defect state versus photon energy for the clean UHV annealed surface and the (4×1)–S superstructure in dependence of the photon energy. The peak positions are at binding energies of 1.1 and 0.8–0.9 eV, respectively.

In the spectra for the clean UHV annealed surface, five peaks were assigned at the binding energies 4.6–4.9 eV (A), 5.4–5.8 eV (B), 6.5–6.9 eV (C), 7.7–8.1 eV (D), and 8.9–9.1 eV (E). These values are close to the peak positions which are found for the defect-free surface after adsorption of O at RT, except for an offset of approximately 0.1–0.2 eV due to band bending as shown in Fig. 2. In Fig. 3(C) the peaks A–E are labeled for the spectrum with a photon energy $h\nu=38.7$ eV. The resonant profiles of these peaks are rather similar to the clean defect-free surface expect for a somewhat higher peak C.

Regardless of the photon energy, the shape of the valence band of the (4×1)–S surface is much less defined than for the clean surface, and a reliable assignment of peak positions as well as the determination of the total number of peaks is not possible. To extract information about the photon energy dependence, the intensity of the upper and lower VB edges around 4.8 and 8.1 eV, respectively, and of the center around 6.3 eV are plotted in Fig. 9(A). The labels a–c in the spectrum at $h\nu=43.4$ eV in Figs. 3(D) and 8(B) mark the energy positions where these data were taken. The defect state (g_1) and the two additional peaks (g_2, g_3) within the band gap can clearly be identified and are labeled in Fig. 8(B) as well as in Fig. 3(D) at a photon energy of 43.4 eV. The heights of these three peaks are plotted against the photon energy in Fig. 9(B). They show maxima at rather low photon energies with a similar resonance profile. In contrast, the three valence-band peaks follow the scheme that lower binding energies exhibit resonances at higher photon energies. The resonance strength was again determined by the ratio of the highest peak height (at resonance) and the peak height at a photon energy at the minimum in the resonance. The values are presented in Fig. 6. The defect state and the two additional peaks in the former band gap exhibit very distinct resonances with the ratio for the peak g_1 being twice as high as the new peaks g_2 and g_3. The resonances of the valence band are not as pronounced as those of the clean surface. Figure 10 shows a direct comparison of the photon energy dependence of the defect state intensity (g_1) of the (4×1)–S surface and the clean UHV annealed surface, respectively. The onset of the resonance differs by approximately 2.4 eV. The resonance for the clean surface is stronger (see Fig. 6) but the overall shape of the two curves is quite similar.

C. Photoemission from the shallow core levels

The influence of sulfur adsorption on the shallow core levels is examined in the overview spectra in Fig. 11. These were taken with a photon energy of 95 eV to monitor the O $2s$ and Ti $3p$ peaks. As mentioned above the saturation coverage for adsorption of S at RT is about 0.7 ML, whereas adsorption on the hot surface leads to saturation coverages of approximately 1 ML. Figure 11(A) compares adsorption of S at RT with adsorption of O at RT on the clean UHV annealed surface. In Fig. 11(B) the spectrum of the clean UHV annealed surface is plotted together with the spectrum after adsorption of S at 350 °C.

In all spectra the shape of the O $2s$ peak has an unusual appearance [arrow in Fig. 11(B)]. It seems to consist of two peaks which are separated from each other by approximately 4.4 eV. The literature values for the O $2s$ and the O $1s$ peak positions are given as 23 and 531 eV, respectively.[32] The XPS O $1s$ binding energies of the clean UHV annealed TiO_2(110) surface was determined as 530.5 eV in previous measurements.[9] The high binding-energy part of the O $2s$ peak of the clean UHV annealed surface is located at 22.5 eV. The offset of 0.5 eV between the value given in Ref. 32 and the measured value of the O $1s$ peak would be consistent to the offset of the O $2s$ position. The origin of the small peak (in our measurements at approximately 18.1 eV) is addressed in Ref. 33. The authors conclude that it represents a satellite of the valence band due to inelastic scattering of photoexcited O $2p$ electrons and it is not correlated to oxygen $2s$ derived emission. To estimate the attenuation of the O

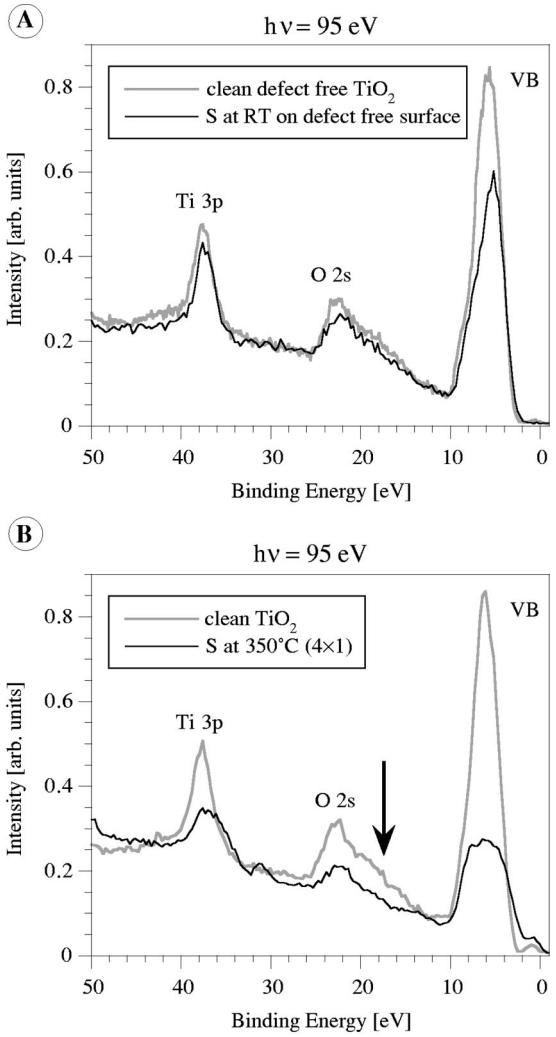

FIG. 11. Photoemission spectra of shallow core levels of $TiO_2(110)$ with $h\nu = 95$ eV. (A) Comparison between oxygen adsorption at RT with sulfur adsorption on the defect-free surface at RT. (B) Comparison between the clean UHV annealed surface and the (4×1)–S superstructure. The O $2s$/Ti $3p$ ratio of the clean surfaces was defined as unity. After adsorption of S at RT it changes to 0.9 and after adsorption at 350 °C to 0.6.

$2s$ peaks of the sulfur covered surfaces we compared therefore only the peak heights of the O $2s$ feature at approximately 22.5 eV.

After adsorption of S at RT (S on the Ti rows) both the oxygen and the titanium peak are slightly attenuated and the peak shapes remain the same. In agreement with the band bending effects observed in the valence-band region, the O $2s$ peak shifts by approximately 0.4–0.5 eV to lower binding energies as compared to the clean UHV annealed surface. The Ti peak exhibits a peak area of approximately 80% of the value for the clean defect-free surface. The oxygen peak height is reduced to approximately 72%. If we define the O/Ti ratio before adsorption as 1, the ratio after adsorption is approximately O/Ti = 0.9. For adsorption of sulfur on the hot surface the oxygen peak height and titanium peak area are attenuated to 42 and 69%, respectively, of the values for the clean UHV annealed surface (with point defects). The O/Ti ratio after adsorption (before adsorption it is again defined as 1) changes to 0.6. The peak shape of the Ti $3p$ peak has changed and a strong low binding-energy shoulder has appeared. The O $2s$ peak of the (4×1)–S structure does not appear to be shifted as compared to the clean, UHV annealed surface.

IV. DISCUSSION

A. Sulfur adsorbed at RT

The photoemission data provide strong arguments for the adsorption of S on point defects at RT as shown in Sec. III A. Another possible explanation for the reduced intensity from the defect state could be an electron transfer from the defects to the S atoms on the Ti rows. However, the following arguments support that the filling of the defects by sulfur is the most probable mechanism. Sulfur replaces bridging oxygen atoms when adsorbed on the hot surface indicating that this position is an energetic favorable adsorption site. Measurements of Cl adsorption on TiO_2 (Ref. 34) exhibit many similarities to the adsorption of S on TiO_2. Cl adsorbs at RT on the Ti rows and replaces bridging oxygen atoms at elevated temperatures. Similar to S, Cl adsorption at RT causes the disappearance of the defect state in photoemission experiments. STM images show adsorption of Cl at defects. Additionally, *ab initio* calculations of Cl on TiO_2 (Ref. 35) reveal that Cl adsorbed on a defect is energetically the most favorable position. As conclusion the photoemission measurement results are pointing to S adsorption at defects, indicating the high reactivity of these sites.

To quench the defect state in the band gap, less sulfur is needed than molecular oxygen. This demonstrates a difference in the adsorption process between oxygen and sulfur. Because molecular oxygen does not adsorb on stoichiometric $TiO_2(110)$ at RT, vacancies are only filled when hit directly by an O_2 molecule. In contrast, sulfur fills the vacancies due to two different processes. Similar to oxygen the vacancies are filled when directly hit by sulfur. Additionally, sulfur sticks to the fivefold coordinated Ti atoms of the stoichiometric $TiO_2(110)$ surface. Sulfur bound to these Ti atoms is very mobile, as seen in STM, and diffuses mainly along the [001] direction.[9] If it passes an oxygen vacancy it can hop into it. The precursor-mediated process naturally accelerates adsorption, and lower doses are required to fill all the defects. The chemical similarity of S and O probably causes a similar appearance in STM when adsorbed on a defect. This inhibits a reliable detection of sulfur on a defect site by STM.

The rigid shift of the valence band displayed in Fig. 2 is readily explained by charge transfer processes and the resulting band bending effects in *n*-type semiconductors.[30] When taking the (approximately) defect-free surface (annealed in UHV and dosed with oxygen at RT) as a reference, the spectrum with defects (before the adsorption of oxygen) is shifted towards higher binding energies by 0.2–0.3 eV. The point defects donate electrons to the substrate, causing an accumulation layer in the near-surface region and downward band bending. This effect is reversed when the defects are filled by either O or S. After dosing S at room temperature, a high

amount of sulfur binds to the surface Ti atoms. Sulfur has a high electronegativity, and is expected to carry a fractional negative charge when adsorbed on TiO_2, thus accepting electrons from the substrate. The resulting depletion in the near-surface carrier concentration leads to an upward bending of the bands by 0.1–0.2 eV as compared to the O-dosed surface, or 0.4 eV as compared to the UHV annealed, defective surface.

All valence-band peaks show resonant behavior for RT adsorption of O as well as of S. The only possible exception is the small shoulder around 3 eV. The resonant photoemission results confirm a hybridization between the titanium and oxygen states in the entire valence band in agreement with the analysis of the clean surface in Refs. 16 and 19 and theoretical calculations.[36] In Refs. 17 and 18 two main resonant processes are described. The Ti $3p-3d$ and the $3p-4s$ excitations are both contributing to the photon energy dependence of Ti-derived valence-band features. Accordingly we find in our measurements a large photon energy range (onset at 34–39 eV to approximately 60 eV) for resonances. The Ti $4s$ level is located at approximately 8 eV above the $3d$ level. Therefore higher photon energies are required for excitation into a $4s$ final state. The tendency for low binding-energy peaks to resonate at higher photon energies confirms a hybridization of this VB region with Ti $4s$ orbitals.[17,18] This tendency was found for all surfaces analyzed in this work. Although the photon energy dependence of the small S shoulder (assigned to a peak around 3.4 eV) was difficult to evaluate, it seems to lack resonant behavior. This would point to a nonhybridized sulfur state at the low binding-energy edge of the VB. Chlorine on TiO_2 adsorbs on the titanium rows at RT, similar to S, and calculations predict a nonhybridized Cl peak close to the VB at the low binding energy (BE) edge.[35] The S shoulder in the spectra could indicate such a peak, provided that the type of bonding is similar. Low energy ion scattering (LEIS) and STM measurements point in this direction.[37] The estimated peak position for this peak around 3.4–3.5 eV fits nicely to the photoemission measurements of $Ti_{1+x}S_2$ in Ref. 27. This paper assigns to emission from mainly sulfur $3p$ orbitals features at 2.2, 3.4, and 5 eV but not at approximately 8 eV where we found additional sulfur-derived features. Since it apparently is not present on a surface composed only of Ti and S it possibly emerges from the interaction of S with oxygen.

B. The TiO_2(110) (4×1)–S superstructure

Adsorption of sulfur on the hot surface gives rise to two new peaks around 2.7 and 3.9 eV [see Figs. 8 and 3(D)] between the defect state g_1 and the upper edge of the valence band. Thus the band gap of the clean TiO_2 is filled. Pure TiS_2 crystals exhibit a band gap of only 0.3 eV.[38] According to the model in Fig. 7 sulfur binds to Ti atoms after replacing the in-plane oxygen atoms. Since the binding energies of the additional peaks are close to the values for emission from S $3p$ in $Ti_{1+x}S_2$ given in Ref. 27, it is reasonable to assign them to levels at least partially derived from S. The resonance behavior of these peaks is similar to the resonance of the defect state [Fig. 9(B)]. Since no resonances exist for S levels in the given photon energy range they are clearly hybridized with Ti $3d$ orbitals.

A rough estimate for the strength of the resonances of different regions in the VB for the various surfaces is given in Fig. 6. To a very first approximation these values can be taken as a qualitative measure for the degree of hybridization with Ti levels. For example, the defect state g_1 on the clean UHV annealed surface shows the strongest resonance of all the features, in agreement with calculations that show that this is a pure Ti $3d$ state.[39] The lower resonance strength of the peaks g_2 and g_3 supports the assumption that these peaks are due to hybridized S $3p$ states and not pure Ti $3d$ orbitals. Additionally, the low resonant photon energy for all the band-gap peaks (g_{1-3}) confirms that these are $3d$-derived states, and are not related to $4s$.

The defect state g_1 is shifted to a 0.2–0.3-eV lower binding energy as compared to the clean UHV annealed surface. This could be caused either by a rigid shift of all peaks due to band bending, or it could represent a property of the (4×1)–S superstructure. The valence band edges are not well enough defined to determine whether band bending takes place, but the O $2s$ peak position seems similar to a clean, defective surface, discounting band bending as a cause for the upwards shift of this peak. There are indications that the shift is an intrinsic effect of the defect state. According to Ref. 40 the defect state of clean TiO_2 moves to lower binding energy when the surface becomes more reduced. This would be the case for the (4×1) superstructure. As seen in the model in Fig. 7, whole rows of oxygens are missing, which leaves the neighboring Ti atoms fourfold coordinated. In comparison, Ti atoms located next to isolated bridging oxygen vacancies are fivefold coordinated, and are expected to have a higher oxidation state than fourfold coordinated Ti atoms. The Ti atoms in the (1×1) rosette structure of TiO_2 (110) (Refs. 41 and 42) are also fourfold coordinated. The defect state of this structure exhibits a shift to lower binding energy similar to one from the (4×1)–S surface while no band bending is found.[43]

Since the surface of the (4×1) superstructure is more reduced than a clean UHV annealed surface, a more intense defect state should be expected. The curves in Fig. 10 for the g_1 defect states of the (4×1)–S structure and the clean surface exhibit a similar total height. However, the strong attenuation of the VB by adsorbed sulfur has to be taken into account when comparing the intensity of the peak for both surfaces. Therefore a similar signal intensity of the Ti $3d$ related defect state for the slightly defective, UHV-annealed surface and for the (4×1)–S superstructure indicates a more reduced surface for the (4×1)–S superstructure. The spectra in Fig. 3(D) give an impression of the large size of the defect-related g_1 peak of the (4×1)–S surface. The high intensity of the g_1 peak stands in agreement with the missing oxygen atoms in the model in Fig. 7. The shifted onset of the defect state resonance of 2.4 eV in Fig. 10 reflects the changes in the environment of the reduced Ti atoms; both the coordination number and the ligands have changed.

A strong attenuation of the Ti $3p$ emission is found upon S adsorption on the hot surface (Fig. 11). Compared to the

clean surface, the Ti $3p$ peak area is reduced to 69% of its original value. This needs to be compared to a reduction to 80% for adsorption at RT. The stronger attenuation is in agreement with the higher sulfur coverage for hot adsorption (1 ML as compared to 0.7 ML). In addition to the sulfur included in the (4×1)–S superstructure, a certain amount of unstructured, excess sulfur is usually present on a saturated hot surface (see the bright spots in the STM image in Fig. 7) and further decreases the ''nonsulfur'' emission.

The O $2s$ peak decreases to 42% of its original value, much more than the Ti $3p$ feature. Furthermore, the peak position of the S $2p$ peak in previous XPS measurements[10] clearly indicates sulfur bonds to Ti and not to oxygen. The strong decrease in the O/Ti ratio (defined as 1 for the clean surface) to 0.6 [for the (4×1)–S superstructure] indicates a decrease in the concentration of surface oxygen, in confirmation of the (4×1)–S model as presented in Fig. 7(B).

The strong Ti shoulder at the low binding-energy side of the Ti $3p$ peak in Fig. 11(B) indicates the presence of Ti^{3+} cations. This is in agreement with previous XPS results[10] which showed a strong Ti^{3+} $2p_{3/2}$ signal, contributing up to 15.6% to the total Ti $2p_{3/2}$ peak area.

The strength of the resonances of the main valence-band peaks are clearly decreased after adsorption of sulfur on the hot surface (see Fig. 6). This could point to a reduced hybridization of the O $2p$ and Ti orbitals, as fewer Ti atoms have O neighbors. It is not clear why the comparatively high emission at 8 eV [peak C in Fig. 6], which was assigned to a contribution of sulfur, exhibits a weak resonance. Definite conclusions cannot be drawn easily because the strength of the resonance is affected by several parameters.[15] Detailed calculations would be necessary to understand the origin of the emission at 8 eV in combination with the resonance behavior.

V. SUMMARY

Normal emission photoemission spectroscopy measurements with photon energies between 29 and 95 eV were analyzed for five differently prepared $TiO_2(110)$ surfaces: the clean UHV annealed surface with surface oxygen vacancies, after adsorption of O_2 at RT on this surface (which fills the vacancies), after adsorption of sulfur at RT on the surface with vacancies, after adsorption of sulfur at RT without the vacancies, and after adsorption of sulfur at 350 °C. Adsorption of S and O at RT on the surface with vacancies causes an upward bending of the bands by 0.4 and 0.2 eV, respectively.

When oxygen adsorbs at RT at the bridging oxygen vacancies the defect state within the band gap totally disappears as expected. Adsorption of S at RT leads to the same result. This indicates that sulfur occupies the reactive oxygen vacancies on the surface, in addition to the adsorption site on fivefold coordinated Ti sites identified with STM. The shape of the valence band is the same when either element, oxygen or sulfur, is occupying the oxygen defects.

After adsorption of S at RT emission from sulfur-derived states was found at approximately 3.4 and 8 eV. As indicated by resonance effects when the photon energy is scanned across the Ti $3p$ ioniziation threshold, the whole valence band (except for the sulfur-related peak at 3.4 eV) is hybridized with Ti states. On both the clean and the S-covered surface, the resonant photon energy depends on the binding energy of valence-band features: the higher the binding energy the higher is the photon energy for resonances. This may indicate a hybridization of the lower binding-energy part of the VB with mainly Ti $4s$ orbitals and of the higher binding-energy part with Ti $3d$ orbitals.

Generally, the valence-band emission after adsorption of sulfur at RT or 350 °C is strongly attenuated. This is caused by the low photoioniziation cross section of the S $3p$ orbitals which, in free atoms, is ten times smaller than for oxygen at the photon energies used in this study.

Sulfur adsorption on the hot surface results in a (4×1) superstructure. Peaks around 2.7 and 3.9 eV are found which can be assigned to sulfur $3p$ orbitals. These resonate at similar photon energies and exhibit a similar profile as the vacancy-derived defect state, indicating a strong hybridization with Ti $3d$ orbitals. The defect state is strongly enhanced and shifts to lower binding energies by 0.3 eV, as it is expected for a more reduced surface. Again a relatively high intensity is found around 8 eV which is assigned to sulfur levels. The oxygen $2s$ peak is strongly reduced due to the removal and partial replacement of surface oxygen by sulfur. The strength of the resonances for the main valence band after sulfur adsorption are clearly decreased, possibly indicating less hybridization with O $2p$ orbitals. The results support the model for the (4×1)–S superstructure proposed in Ref. 10 and depicted in Fig. 7.

ACKNOWLEDGMENTS

This work was supported by NSF-CAREER (Tulane), the Louisiana Board of Regents (UNO), and U.S. DOE (No. DE-FG02-98ER45712) (CAMD).

[1] J. A. Rodriguez, S. Chaturvedi, M. Kuhn, and J. Hrbek, J. Phys. Chem. B **102**, 5511 (1998).
[2] J. A. Rodriguez and J. Hrbek, Acc. Chem. Res. **32**, 719 (1999).
[3] K. E. Smith and V. E. Henrich, Phys. Rev. B **32**, 5384 (1985).
[4] K. E. Smith, J. L. Mackay, and V. E. Henrich, Phys. Rev. B **35**, 5822 (1987).
[5] K. E. Smith and V. E. Henrich, Surf. Sci. Lett. **217**, L445 (1989).
[6] K. E. Smith and V. E. Henrich, J. Vac. Sci. Technol. A **7**, 1967 (1989).
[7] D. R. Warburton, D. Purdie, C. A. Muryn, K. Prabhakaran, P. L. Wincott, and G. Thornton, Surf. Sci. **269/270**, 305 (1992).
[8] H. Raza, S. P. Harte, C. A. Muryn, P. L. Wincott, G. Thornton, R. Casanova, and A. Rodriguez, Surf. Sci. **366**, 519 (1996).
[9] E. L. D. Hebenstreit, W. Hebenstreit, and U. Diebold, Surf. Sci.

461, 87 (2000).
[10] E. L. D. Hebenstreit, W. Hebenstreit, and U. Diebold, Surf. Sci. **470**, 347 (2001).
[11] U. Diebold, J. Lehman, T. Mahmoud, M. Kuhn, G. Leonardelli, W. Hebenstreit, M. Schmid, and P. Varga, Surf. Sci. **411**, 137 (1998).
[12] J. A. Rodriguez, J. Hrbek, J. Dvorak, T. Jirsak, and A. Maiti, Chem. Phys. Lett. **336**, 377 (2001).
[13] P. J. Hardman, G. N. Raikar, C. A. Muryn, G. van der Laan, P. L. Wincott, G. Thornton, D. W. Bullett, and P. A. D. M. A. Dale, Phys. Rev. B **49**, 7170 (1994).
[14] G. N. Raikar, P. J. Hardman, C. A. Muryn, G. van der Laan, P. L. Wincott, and G. Thornton, Solid State Commun. **80**, 423 (1991).
[15] L. C. Davis, J. Appl. Phys. **59**, R25 (1985).
[16] E. Bertel, R. Stockbauer, R. L. Kurtz, T. E. Madey, and D. E. Ramaker, Surf. Sci. **152/153**, 776 (1985).
[17] R. Heise, R. Courths, and S. Witzel, Solid State Commun. **84**, 599 (1992).
[18] Z. Zhang, S.-P. Jeng, and V. E. Henrich, Phys. Rev. B **43**, 12 004 (1991).
[19] J. Nerlov, Q. Ge, and P. J. Møller, Surf. Sci. **348**, 28 (1996).
[20] K. C. Prince, V. R. Dhanak, P. Finetti, J. F. Walsh, R. Davis, C. A. Muryn, H. S. Dhariwal, G. Thornton, and G. van der Laan, Phys. Rev. B **55**, 9520 (1997).
[21] U. Diebold, H.-S. Tao, N. D. Shinn, and T. E. Madey, Phys. Rev. B **50**, 14 474 (1994).
[22] S. Fischer, F. Schneider, and K. D. Schierbaum, Vacuum **47**, 1149 (1996).
[23] S. Fischer, J. A. Martín-Gago, E. Román, K. D. Schierbaum, and J. L. de Segovia, J. Electron Spectrosc. Relat. Phenom. **83**, 217 (1997).
[24] P. J. Møller, Z. S. Li, T. Egebjerg, M. Sambi, and G. Granozzi, Surf. Sci. **402-404**, 719 (1998).
[25] J. Biener, M. Bäumer, and R. J. Madix, Surf. Sci. **432**, 178 (1999).
[26] K. E. Smith and V. E. Henrich, Phys. Rev. B **38**, 9571 (1988).
[27] Y. Ueda, H. Negishi, M. Koyano, M. Inoue, K. Soda, H. Sakamoto, and S. Suga, Solid State Commun. **57**, 839 (1986).
[28] W. Heegemann, K. H. Meister, E. Bechtold, and K. Hayek, Surf. Sci. **49**, 161 (1975).
[29] M. A. Henderson, W. S. Epling, C. L. Perkins, C. H. F. Peden, and U. Diebold, J. Phys. Chem. B **103**, 5328 (1999).
[30] V. E. Henrich and P. A. Cox, *The Surface Science of Metal Oxides* (Cambridge University Press, Cambridge, England, 1994).
[31] J. J. Yeh and I. Lindau, At. Data Nucl. Data Tables **32**, 1 (1985).
[32] J. F. Moulder, W. F. Stickle, P. E. Sobol, and K. D. Bomben, *Handbook of X-ray Photoelectron Spectroscopy* (Perkin-Elmer Corporation, Physical Electronics Division, Eden Prairie, MN, 1992).
[33] K. W. Goodman and V. E. Henrich, Phys. Rev. B **50**, 10 450 (1994).
[34] E. L. D. Hebenstreit, W. Hebenstreit, H. Geisler, C. A. Ventrice, Jr., and P. T. Sprunger, Surf. Sci. **486**, L467 (2001).
[35] D. Vogtenhuber, R. Podloucky, and J. Redinger, Surf. Sci. **454-456**, 369 (2000).
[36] C. Sousa and F. Illas, Phys. Rev. B **50**, 13 974 (1994).
[37] W. Hebenstreit, E. L. D. Hebenstreit, D. Vogtenhuber, and U. Diebold (unpublished).
[38] C. H. Chen, W. Fabian, F. C. Brown, K. C. Woo, B. Davies, and B. DeLong, Phys. Rev. B **21**, 615 (1980).
[39] P. J. D. Lindan, N. M. Harrison, M. J. Gillan, and J. A. White, Phys. Rev. B **55**, 15 919 (1997).
[40] V. E. Henrich, G. Dresselhaus, and H. J. Zeiger, Phys. Rev. Lett. **36**, 1335 (1976).
[41] M. Li, W. Hebenstreit, and U. Diebold, Surf. Sci. Lett. **414**, L951 (1998).
[42] M. Li, W. Hebenstreit, L. Gross, U. Diebold, M. A. Henderson, D. R. Jennison, P. A. Schultz, and M. P. Sears, Surf. Sci. **437**, 173 (1999).
[43] H. Geisler, C. A. Ventrice, Jr., W. Hebenstreit, E. L. D. Hebenstreit, P. T. Sprunger, and U. Diebold (unpublished).